Hindawi
Advances in Materials Science and Engineering
Volume 2018, Article ID 4231571, 7 pages
https://doi.org/10.1155/2018/4231571

Research Article

Synthesis of Copper Oxide Aided by Selective Corrosion in Cu Foils

Roberto Baca Arroyo

Department of Electronics, National Polytechnic Institute, 07738 Mexico City, Mexico

Correspondence should be addressed to Roberto Baca Arroyo; rbaca02006@yahoo.com.mx

Received 14 August 2017; Revised 5 December 2017; Accepted 31 December 2017; Published 19 February 2018

Academic Editor: Alicia E. Ares

Copper oxide films aided by selective corrosion have been synthesized. Using copper (Cu) foils of commercial printed circuit boards (PCBs), chemical attack in small areas on Cu surfaces and their oxidation with heating process in air atmosphere at low temperature have allowed to produce Cu oxide layers. Phase formation of Cu oxide samples was validated by X-ray diffraction studies, and their conduction properties were registered and evaluated by current-voltage curves. Stability analysis of the Cu oxide samples was conducted by a correlation profile between average strain and Cu oxide percentage grown, which confirms that the structure defects dependent on plastic deformation define the existence of both CuO and Cu_2O phases beneficial to mitigate corrosion and advance in Cu oxide-based devices to build electronic circuits as components on PCBs.

1. Introduction

It is well known that copper (Cu) is a nature-abundant material and is the third metal more employed in the world, after iron and aluminum. It has an important biological role in photosynthesis, and it is essential for human life. Despite the standard negative electrode potential with −0.345 V, its corrosion can occur at a significant rate under strenuous conditions [1]. Both cupric oxide (CuO) and cuprous oxide (Cu_2O) are the two chemical compounds formed by oxygen and copper in the nature only. Such oxides are semiconductors, where Cu_2O has a direct bandgap of 2.1 eV and reddish appearance, while CuO with a bandgap of 1.3 eV is black in color [2].

Due to the miniaturization in the integrated circuits (ICs), Cu has been widely used for microelectronic device industry, including wiring technology, electromagnetic interference shielding, and electrostatic dissipation technology [3]. However, the reduced spacing between IC components on a printed circuit board (PCB) can produce various types of corrosions, although the underlying mechanism in all cases has been electrochemical migration (EM) as one of the most severe problems, where events such as temperature cycles during soldering at temperature above 150°C, degradation of the thermal interface in contacts, existence of dust particles between contacts, and application of high voltage for operation of the electronic devices have made it easy for corrosive environments [4, 5]. The high-temperature corrosion occurs when gradual EM by Cu ions along an interconnection under high current density (current crowding) increases the resistance of the Cu lines with reduction in their cross-sectional area [6]. High-temperature corrosion can be able to assist the oxidation in the Cu lines where their surface will remain safe, and small fluctuations will degrade the oxide in few critical points due to the pit formation under humidity conditions. The interior of a pit is naturally poorer in oxygen, and pH locally decreases to very low values, thus pitting corrosion increase due to the catalytic process where dendrite growth from cathode to anode produces an electric short and premature failure. Figure 1 shows pitting corrosion and dendrite growth on a PCB when high electric field was applied [7].

Previously, studies have shown that for maximizing reliability in IC design and PCB fabrication, width scaling of Cu lines must be investigated by EM phenomena where to reduce failures by corrosion environments, two scenarios

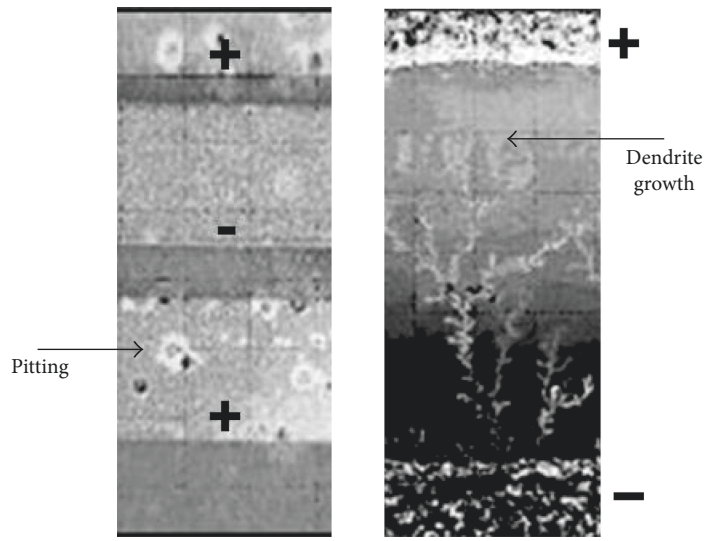

Figure 1: Corrosion phenomena on a PCB based on EM under high electric field conditions.

have been recommended with respect to the mechanisms governing the Cu ion migration with the suggested spacing between IC components satisfying a width <1 μm, whereas a width >1 μm is for components on PCBs [6, 8].

Nowadays, researchers have synthesized p-channel Cu_2O thin-film transistors on flexible polyethylene terephthalate (PET) substrates by using magnetron sputtering and vacuum annealing techniques [9, 10]. Such novel electronic devices provide modest transport properties with hole mobility (μ_h) in the range of 1 to 10 cm^2/Vs and hole concentration (n_h) from 10^{16} to 10^{17} cm^{-3}. Its conduction mechanism is attributed to the electronic structure of intrinsic defects such as Cu vacancies [V_{Cu}], which create trap states [11]. Conversely, the operation characteristics of the Cu_2O thin-film transistors are of no use today to engineering applications, and the market for Cu_2O-based devices has been delayed by setback in its scalability, degradation of their electronic properties at high-temperature conditions, and requirements for high quality of Cu_2O with a minimum in structure defects. Consequently, to achieve useful engineering applications using Cu oxide-based devices compatible with silicon technology and controllable operation characteristics, the formation and growth of CuO on the Cu surface can increase the chemical bonding and path of the specific thermal resistance in Cu_2O-based devices for electronic circuits designed as components on PCBs [5]. The layer CuO is accompanied by defects such as dislocations and grain boundaries where reactivity of these is dependent on intrinsic structure disorder (elastic strain effects) [12]. Thus, transformation in the microstructure of the Cu surface (process known as plastic deformation) can be a strategy to adjust defect density and mitigate corrosion issues [3].

In the past, oxidation procedures at high temperature around 1000°C in air atmosphere have been developed to oxidize Cu foils in order to obtain polycrystalline Cu_2O crystals [11], where Cu oxidation has taken place by diffusion process of the Cu ions which migrate because there is an opposite diffusion of [V_{Cu}] from oxide layer to the Cu foil [1]. Nevertheless, as CuO is less stable than Cu_2O and its formation energy is lower, the presence of CuO appearing together with Cu_2O can be attained by plastic deformation on the Cu surface at low temperatures [2, 4]. Thereby, the work presents the synthesis of Cu oxide films aided by selective corrosion of Cu foils with the subsequent heating process in air atmosphere at low temperatures. Such experimental procedure will be discussed in Section 2. Phase formation and conduction properties in Cu oxide films and stability analysis as a function of average elastic strain originated by selective corrosion will be covered in Section 3. Conclusions about this research are presented in Section 4.

2. Experimental Procedure

Cu foils with an average thickness of 15 μm were obtained from commercial PCBs with copper joined in a fiberglass epoxy polymer. Before, Cu foils were cut in a cross-sectional area of 1 cm^2; after, cleaning process to remove nonpolar substances was developed with acetone; finally, washing process was completed in deionized water and successively dried with nitrogen. In the synthesis of Cu oxide aided by selective corrosion, the following four stages are involved: (a) choosing the area for chemical attack, (b) immersing Cu foils in $FeCl_3/H_2O$ solution, (c) removing residual $FeCl_3/H_2O$ by soaking the chemically attacked Cu foils, and (d) heating the Cu foils in air atmosphere inside of quartz tube furnace. Figure 2 shows the stages in the synthesis to obtain Cu oxide films.

A nontoxic permanent marker typically engaged in the design of PCBs was used to synthesize Cu oxide samples. An area of 4 mm × 4 mm was defined on each Cu foil under study. A permanent marker is resistant at $FeCl_3/H_2O$ solution; therefore, during corrosion, the outside area was protected as shown in Figure 2. Iron chloride ($FeCl_3$) solution activated with H_2O was employed as the electrolyte.

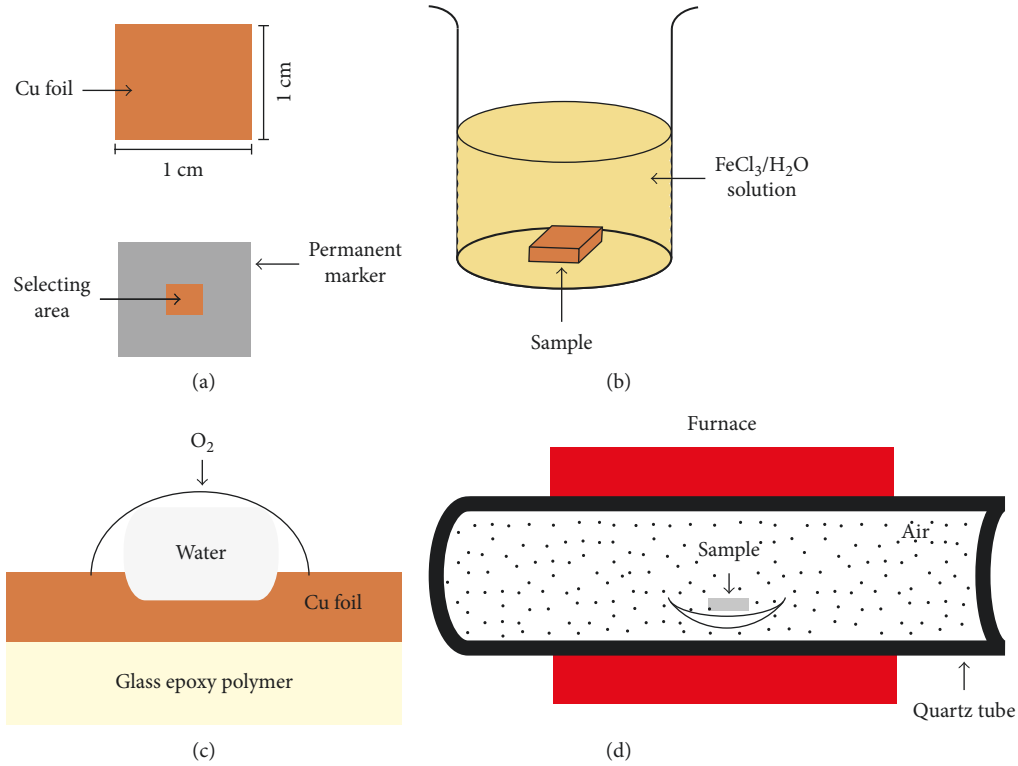

Figure 2: Stages employed in the synthesis of Cu oxide films.

The corrosion behavior by chemical attack was studied at different $FeCl_3 : H_2O$ rates and immersion times as indicated in Table 1.

The reaction mechanism for Cu corrosion can be written in two stages as

$$FeCl_3/H_2O\,(aq) + Cu\,(s) \rightarrow FeCl_2\,(aq) + CuCl\,(s) \quad (1)$$

$$FeCl_3/H_2O\,(aq) + CuCl\,(s) \rightarrow FeCl_2\,(aq) + CuCl_2\,(s) \quad (2)$$

The species dissolved in $FeCl_3$ activated with H_2O are $Fe^{2+}Cl_2^-$, $Fe^+(OH)^-$, and H^+Cl^- which indicate that corrosion in Cu foils occur because initially Cu^+ ion in the presence of H^+ ion produces cupric chloride (CuCl), and later cuprous chloride ($CuCl_2$) is fully formed by the reaction of CuCl with Cu^{2+} ion [1, 13, 14].

Once Cu foils were immersed in the $FeCl_3/H_2O$ solution to obtain $CuCl_2$ and soaked with water, heating process at 35°C with a duration of 2 min at atmospheric pressure was completed. In accordance with the following reaction mechanism, the formation of Cu oxide films took place in two stages:

$$2CuCl_2 + O_2 + 2H_2O \rightarrow 2Cu\,(OH)\,(aq) + 2HCl\,(aq) + O_2 \quad (3)$$

$$Cu^+(OH)^- + H^+Cl^- + \frac{1}{2}O_2^{2-} \xrightarrow{\text{heat}} Cu_xO_{1-x}\,(\text{oxide}) + H_2O \quad (4)$$

where x is the chemical composition in Cu oxide samples.

Table 1: Parameters for selective corrosion in Cu foils.

Sample	Volume (mL)		Immersion time (min)
	$FeCl_3$	H_2O	
CS-1	5	2.5	2
CS-2	2.5	2.5	4
CS-3	2.5	5	6

The heating temperature for the Cu samples was chosen as a function of the boiling point for HCl of 48°C, where Cl^- ions and residual water are fully evaporated. The surface of Cu oxide samples resulted with opaque gray color after thermal process. The presence of ionic species such as copper hydroxide (CuOH) and acidic chloride (HCl) determines the oxidation degree of the $CuCl_2$ surfaces because displacement interactions between OH^- and H^+ ions initially synthetize CuO by surface migration of such ionic species and after Cu_2O by diffusion of Cu^+ ions and reaction with atmospheric oxygen [3, 14]. Nevertheless, as the activity of these species is poorer under heating process within humidity, the Cu oxide films were nonstoichiometric.

Using X-ray diffraction with PANalytical diffractometer of CuK_α radiation ($\lambda = 0.1541$ nm), phase formation of Cu oxide films was validated. Conduction behavior in the samples was registered and evaluated by current-voltage curves at room temperature. The electrical parameters of the samples were collected by employing a digital storage oscilloscope (Tektronix, TDS1012C). To know the performance of the Cu oxide samples as a function of structure

defects involved, a stability analysis was done by a correlation profile between elastic strain and Cu oxide percentage.

3. Results and Discussion

This section discusses phase formation and conduction properties in the Cu oxide samples. Here are the revised XRD patterns and electrical characterization to demonstrate the potential of the selective corrosion technique with emphasis in the oxidation degree of the Cu foils dependent on their plastic deformation.

3.1. X-Ray Diffraction in Cu Oxide Samples. Figure 3 shows XRD patterns of Cu oxide films synthesized with the heating process. The samples labeled as CS-1, CS-2, and CS-3 exhibit monoclinic phase (CuO) with peaks located at 33.9° and plane (110), 58.1° and plane (202), and 65.2° and plane (022) according to PANalytical Card number 00-041-0254. Also, peak positioned at 69.7° and plane (310) corresponds to cubic phase (Cu_2O) according to PANalytical Card number 00-005-0667. As a reference, the XRD pattern of Cu foil also is shown. The larger peak-position displacement between XRD patterns of the Cu oxide films and XRD pattern of the Cu foil was observed which ensures presence of the elastic strain in Cu oxide surface induced by high density of the defects in chemically attacked Cu foils.

3.2. Conduction Properties in Cu Oxide Samples. The performance of Cu oxide samples has been confirmed with the schematic diagram of Figure 4(a). To ensure linear response, a function generator (Matrix, MFG-8250A) was used to produce a linear ramp signal at low frequency ($f = 100$ Hz) with voltage ranging from -2 V to 2 V to conserve low-voltage operation across the aluminum (Al) contacts. Also, a resistor of $R = 1\,\text{k}\Omega$ was chosen to monitor the current signal. The log current-voltage plots for samples labeled as CS-1, CS-2, and CS-3 are shown in Figure 4(b), where such current-voltage curves have shown ohmic behavior.

To investigate conduction parameters, a model based on the point form of Ohm's law [15] has been proposed by

$$\frac{\Delta V}{\Delta I} = \frac{l_c}{\sigma_o \exp\left(-\left(E_a/k_B T\right)\right) \cdot S}, \tag{5}$$

where $\sigma_o = 5.8 \times 10^5 \Omega^{-1}\text{cm}^{-1}$ is the Cu conductivity at room temperature, E_a is the activation energy of Cu oxide, k_B is the Boltzmann constant, T is the temperature in samples under test, $l_c = 0.77$ nm is the interatomic distance into CuO crystalline lattice associated with minimal free path of charge carries [16], and S is the cross-sectional area ($S = t \cdot d$), where $d = 0.5$ mm is the diameter of aluminum (Al) contact and t the thickness of the samples.

The $\Delta V/\Delta I$ rate was extracted from Figure 4(b), with ΔV as the differential voltage and ΔI as the differential current, respectively, while E_a was estimated with the slope of the dotted line in Figure 4(b) which crosses at the voltage axis. Using MATLAB program, the cross-sectional area $S = t \cdot d$ is computed by solving (5) and by the Arrhenius conductivity dependent on temperature [17]. $[V_{Cu}]$ was estimated by

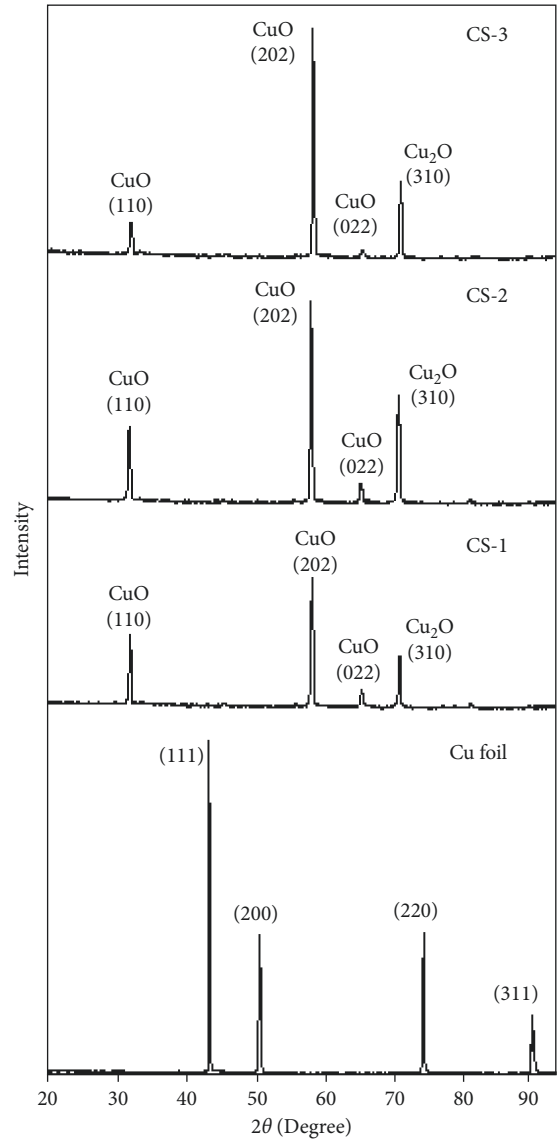

Figure 3: XRD patterns in Cu oxide films grown on Cu foils.

$$[V_{Cu}] \cdot e \cdot \mu_{Cu} = \sigma_o \exp\left(-\frac{E_a}{k_B T}\right), \tag{6}$$

where $\sigma_s(E_a) = [V_{Cu}] \cdot e \cdot \mu_{Cu}$ is the conductivity for the Cu oxide layer, while μ_{Cu} corresponds to the mobility of Cu vacancies. The quantity $[V_{Cu}]\mu_{Cu}$ from (6) was computed, confirming that $[V_{Cu}]$ is attained in the range of 10^{14} to $10^{15}\,\text{cm}^{-3}$ and mobility from 1 to $40\,\text{cm}^2/\text{Vs}$, which confirms that the operation characteristics in Cu oxide samples would be useful in engineering applications because their specific thermal resistance chemically controlled by CuO and electronic properties driven by Cu_2O allow advances in design of Cu oxide-based devices whose principle of operation similarly to previous studies by other authors is dependent on strain effects [18, 19]. Table 2 summarizes the conduction parameters found.

3.3. Stability in Cu Oxide Samples. To evaluate the performance of the Cu oxide samples as a function of the plastic

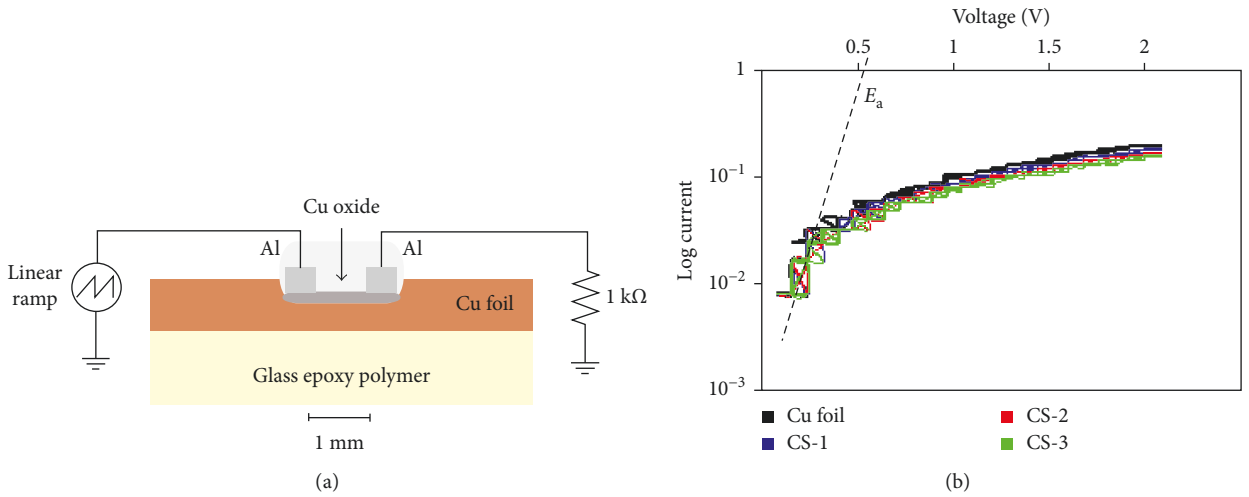

Figure 4: (a) Schematic diagram of practical circuit implemented to measure the current-voltage curves in Cu oxide samples. (b) Log current-voltage plots of each sample.

Table 2: Conduction parameters in Cu oxide samples.

Sample	E_a (eV)	$\Delta V/\Delta I(\Omega)$	$\sigma_s(E_a)\cdot(\Omega^{-1}\cdot cm^{-1})$	t (nm)	$\mu\cdot[V_{Cu}]\cdot(cm^{-1}\cdot V^{-1}\cdot s^{-1})$
CS-1	0.54	130.43	5.55×10^{-4}	212.1	3.5×10^{15}
CS-2	0.56	190.47	2.57×10^{-4}	314.6	1.6×10^{15}
CS-3	0.56	315.78	2.57×10^{-4}	189.7	1.6×10^{15}

deformation in Cu foils, average strain along each crystallographic plane on the oxidized Cu surface with respect to the Cu foil as substrate is approximately estimated by $(\Delta d/d) = \Delta\theta/\tan\phi$ [12], where $\Delta\theta$ is the difference between measured incident angle θ_m and reference angle θ_r, while the angle of each Cu foil plane corresponds to ϕ. The parameter $(x \approx \Delta d/d)$ can be linked with the chemical composition in Cu_xO_{1-x} which defines its nonstoichiometry [20].

The elastic strain must be analyzed as a function of Cu oxide grown, being it proportional to the intensity in percentage of each peak [12, 20]. Figure 3 allows evaluating $\Delta\theta$ at each crystallographic plane of both oxides (Cu_2O and CuO), as well as $\tan\phi$ at each crystallographic plane in the Cu foil; thus, a correlation profile between x and Cu oxide percentage is built in Figure 5.

The structure defects can be validated by stability analysis, which determines the ability of the Cu oxide layers to remain structurally stable during electrical conduction. The stability in the Cu oxide samples is a function of both tensile and compressive stress into a limit where Cu oxide (Cu_xO_{1-x}) is fully grown into two phases. In Figure 5, both oxides (Cu_2O and CuO) give a slight deviation from their nonstoichiometry into the range of $-1 < x < 1$, which corresponds to the limit where the Cu oxide percentage from 30 to 100% is stable. In contrast, anomalous Cu oxide is lower than30%, because its severe nonstoichiometry is associated with intergranular local attack influenced by poor quality of the initial Cu surface.

Selective corrosion followed with the heating process at 35°C had allowed obtaining both Cu_2O and CuO phases in accordance with the experimental procedure detailed in Section 2, where oxidation in Cu foils occurs beginning with a first layer of CuO grown on Cu, and subsequently a layer of Cu_2O grows between Cu and CuO. These two layers increase with time because the Cu_2O has a very small expansion coefficient at lower temperatures of 300°C where the lattice constant changes to less than 0.5% and the dissociation pressure of CuO is lower than the atmospheric pressure [11, 13]. As Cu vacancies agglomeration or trapped oxygen happen into grain boundaries, intrinsic concentration of defects corresponding with $[V_{Cu}]$ and the opaque gray color in Cu oxide samples explicate the stability of the CuO phase.

4. Conclusions

Cu oxide samples synthesized by corrosion and heating processes at low temperature have been studied. Selective corrosion was achieved by chemical attack in smaller areas from Cu foils of commercial PCBs. Both CuO and Cu_2O phases were formed under air atmosphere. The study conducted by X-ray diffraction and electrical characterization found that phase formation and conduction properties are linked with structure defects into Cu foils. Stability analysis has confirmed that the structure behavior in Cu oxide samples is strongly dependent on its intrinsic disorder. Thus, the selective corrosion technique has significant benefits as physical and mechanical properties are influenced by plastic deformation, which has resulted in stable Cu oxide samples with next electronic engineering applications for Cu oxide-based devices.

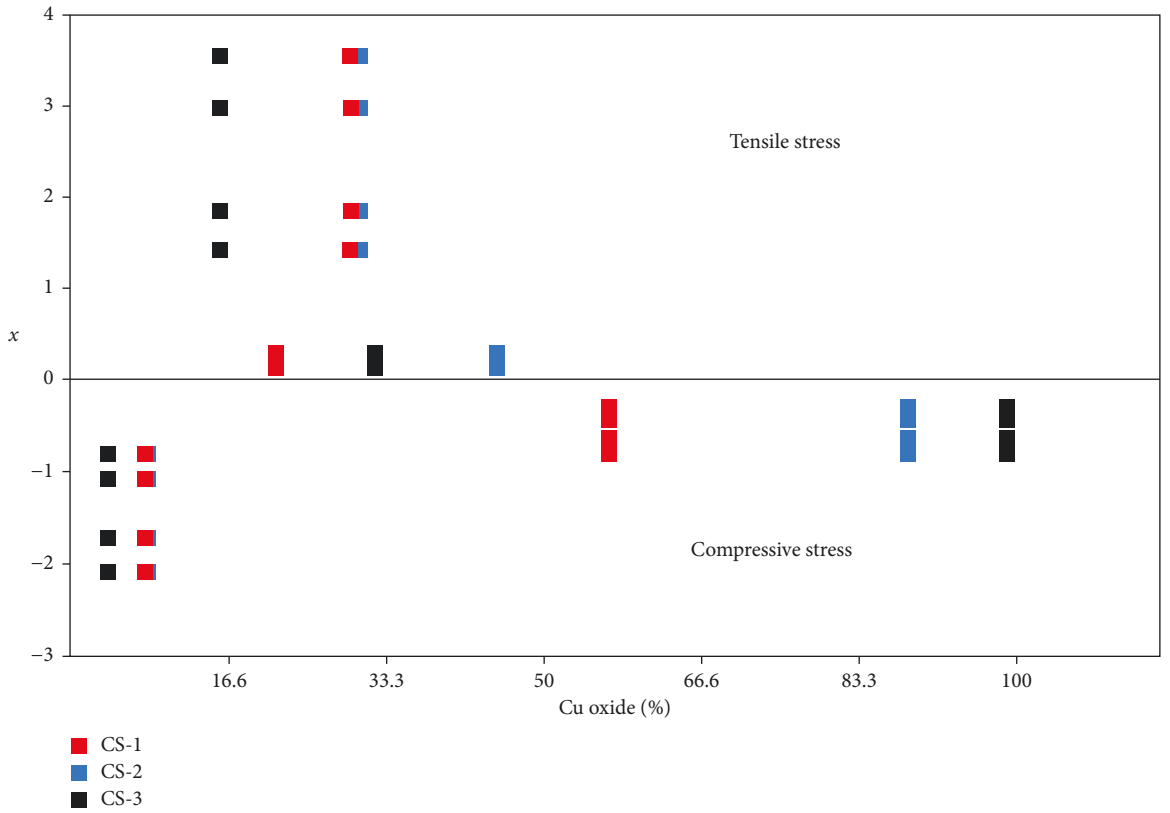

Figure 5: Correlation profile for different Cu oxide samples.

Conflicts of Interest

The author declares that there are no conflicts of interest, but there is an interest regarding the publication of this manuscript to share knowledge about green material processing and their applications.

Acknowledgments

The structural data collected from XRD studies have been supported thanks to Dr. José Alberto Andraca Adame from CNMN belonging at the National Polytechnic Institute, Mexico City, Mexico.

References

[1] A. C. Keyser, *Materials Science in Engineering*, Prentice Hall, Inc., México City, Mexico, 6th edition, 1990.

[2] L. Y. Isseroff and E. A. Carter, "Electronic structure of pure and doped cuprous oxide with copper vacancies: suppression of trap states," *Chemistry of Materials*, vol. 25, no. 3, pp. 253–265, 2013.

[3] W. Deng, P. Lin, Q. Li, and G. Mo, "Ultrafine-grained copper produced by machining and its unusual electrochemical corrosion resistance in acidic chloride pickling solutions," *Corrosion Science*, vol. 74, pp. 44–49, 2013.

[4] J.-M. Song, D.-S. Wang, C.-H. Yeh, W.-C. Lu, Y.-S. Tsou, and S.-C. Lin, "Texture and temperature dependence on the mechanical characteristics of copper electrodeposits," *Materials Science and Engineering A*, vol. 559, pp. 625–644, 2013.

[5] R. Skuriat, J. F. Li, P. A. Agyakwa, N. Mattey, P. Evans, and C. M. Johnson, "Degradation of thermal interface materials for high-temperature power electronics applications," *Microelectronics Reliability*, vol. 53, no. 12, pp. 1933–1942, 2013.

[6] Md. K. Rahman, A. M. M. Musa, B. Neher, K. A. Patwary, M. A. Rahman, and Md. S. Islam, "A review of the study on the electromigration and power electronics," *Journal of Electronics Cooling and Thermal Control*, vol. 6, no. 1, pp. 19–31, 2016.

[7] G. S. Frankel, *Corrosion Mechanisms in Theory and Practice*, Marcel Dekker, New York, NY, USA, 1995.

[8] M. H. Lin, K. P. Chang, K. C. Su, and T. Wang, "Effects of width scaling and layout variation on dual damascene copper interconnect electromigration," *Microelectronics Reliability*, vol. 47, no. 12, pp. 2100–2108, 2007.

[9] Z. Q. Yao, S. L. Liu, L. Zhang et al., "Room temperature fabrication of p-channel Cu_2O thin-film transistors on flexible polyethylene terephthalate substrates," *Applied Physics Letters*, vol. 101, no. 4, p. 042114, 2012.

[10] J. Yu, G. Liu, A. Liu, Y. Meng, B. Shin, and F. Shan, "Solution-processed p-type copper oxide thin-film transistors fabricated by using a one-step vacuum annealing technique," *Journal of Materials Chemistry C*, vol. 3, no. 37, pp. 9509–9513, 2015.

[11] N. Cabrera and N. F. Mott, "Theory of the oxidation of metals," *Reports on Progress in Physics*, vol. 12, no. 1, pp. 163–184, 1949.

[12] P. F. Fewster, *X-Ray Scattering from Semiconductors*, Imperial College Press, Singapore, 2nd edition, 2003.

[13] A. Cotton and G. Wilkinson, *Advanced Inorganic Chemistry*, John Wiley & Sons, New York, NY, USA, 4th edition, 2008.

[14] M. Ottosson, M. Boman, P. Berastegui et al., "Copper in ultrapure water, a scientific issue under debate," *Corrosion Science*, vol. 122, pp. 53–60, 2017.

[15] A. S. Grove, *Physics and Technology of Semiconductor Devices*, John Wiley & Sons, New York, NY, USA, 1st edition, 1967.
[16] M. Lundstrom, *Fundamentals of Carrier Transport*, Cambridge University Press, New York, NY, USA, 2nd edition, 2000.
[17] J. J. O'Dwyer, *The Theory of Electrical Conduction and Breakdown in Solid Dielectrics*, Clarendon Press, Oxford, UK, 1st edition, 1973.
[18] R. K. Zheng, C. Chao, H. L. W. Chan, C. L. Choy, and H. S. Luo, "Converse piezoelectric control of the lattice strain and resistance in $Pr_{0.5}Ca_{0.5}MnO_3$/PMN-PT structures," *Physical Review B*, vol. 75, no. 2, p. 024110, 2007.
[19] V. P. Malinenko, L. A. Aleshina, A. L. Pergament, and G. V. Germak, "Switching Effects and Metal-Insulator Transition in Manganese Oxide," *Journal on Selected Topics in Nano Electronics and Computing*, vol. 1, no. 1, pp. 44–50, 2013.
[20] R. Baca-Arroyo, "Structural characterization of the chromium-iron alloy formed by thermal diffusion processes," *Advanced Materials Research*, vol. 651, pp. 284–288, 2013.